Scientia Iranica (2024) 31(7), 541–555

Sharif University of Technology
Scientia Iranica
Transactions A: Civil Engineering
https://scientiairanica.sharif.edu

The effect of dolphin echolocation-fuzzy logic controller in semi-active control of structural systems using endurance time method

F. Moghadam-Rad[a], P. Zarfam[a,*], and M. Zabihi-Samani[b]

a. *Department of Civil Engineering, Science and Research Branch, Islamic Azad University, Tehran, Iran.*
b. *Department of Civil Engineering, Parand Branch, Islamic Azad University, Tehran, Iran.*

Received 2 December 2020; received in revised form 15 September 2022; accepted 18 January 2023

KEYWORDS
Semi-active control of smart buildings;
Fuzzy logic control;
Dolphin Echolocation (DE);
Magnetorheological damper;
Endurance Time Analysis (ETA).

Abstract. An adaptive Fuzzy Logic Controller (FLC) is proposed to actuate MR damper smartly. Minimizing the excessive responses of buildings should be considered as a multi-objective optimization problem. The new-generation structural systems should be designed based on the seismic performance level. Designing based on performance requires dynamic, heavy, and repetitive time history analyses. The Endurance Time Analysis method (ETA) is a modern dynamic method based on the performance of the structure, which leads to the reduction of time and number of structural analyses. To investigate the efficiency of Dolphin Echolocation-Fuzzy Logic Controller (DE-FLC) and ETA, several ET simulations were performed. The seismic responses of 11th-story benchmark building equipped with MR dampers were investigated in two cases of seven time-history analysis and six-generation ET functions. By using dolphin echolocation, the optimal arrangement and the number of sensors and dampers are determined. The proposed DE-FLC controller exhibits its efficiency by reducing the excessive displacement under seismic excitations in comparison with the uncontrolled case and classical FLC. Furthermore, the results demonstrate that the sixth generation of ETA can simulate responses of several time-history analyses well with proper accuracy, without necessitating any computational burden.

1. Introduction

To ensure the life usability and reliability of structural systems, dissipation of excessive vibration from natural hazards is crucial. Control systems have been utilized as one of the most promising technologies in structural design. A modern controller can be applied to new-generation buildings to diminish undesired responses [1]. A passive, semi-active, active, and hybrid control devices were introduced and utilized [2]. Performances of passive control devices are admissible; however, incompatibility with undesirable vibration conditions is the most serious problem in robustness and efficiency of the building with this equipment

*. *Corresponding author.*
E-mail addresses: farzammr@yahoo.com (F. Moghadam-Rad); zarfam@srbiau.ac.ir (P. Zarfam); mzabihi@iust.ac.ir (M. Zabihi-Samani)

To cite this article:
F. Moghadam-Rad, P. Zarfam, and M. Zabihi-Samani "The effect of dolphin echolocation-fuzzy logic controller in semi-active control of structural systems using endurance time method", *Scientia Iranica* (2024), **31**(7), pp. 541-555
DOI: 10.24200/sci.2023.57268.5147

pieces. Active control devices have been introduced and designed, but they require further development to dissolve energy consumption during excitations and robustness obstacles [3].

With the advent of smart fluids, semi-active devices have been utilized in buildings. A semi-active control system does not use any external force in the structural system. Several studies have managed to develop proprietary control algorithms that could enhance the unique characteristics of MR fluids [4]. In smart structural systems, MR dampers are new semi-active control devices that could enhance the vibration control technology [5]. MR dampers enjoy the reliability of passive control devices concurrent with the versatility and adaptability of active control devices. They contain a semi-fluid in the piston that could change the "shock" energy into heat by transferring the fluids between two different chambers via tiny orifices. By transmitting the electrical current, a coil inside the piston constructs a magnetic field and modifies the characteristics of the MR fluid. Therefore, the resistance of the damper can be continuously modified online by modulating electrical current to the damper fluids, instantaneously. Large-scale MR dampers have been fabricated, and several full-scale structures have utilized semi-active devices to reduce the undesirable vibration responses [6–8].

To formulate the mechanical behavior of MR dampers, Bouc-Wen hysteresis model has been proposed [9]. The application of MR damper in structural systems is more progressive and the economical parameters should be considered in an optimized controller. Different control levels could be utilized by changing the arrangement of dampers. Hence, optimal damper arrangement should be accomplished. Furthermore, it is important to reduce the cost of purchase, installation, operation, and maintenance of the semi-active devices [10]. Several researches have investigated the optimal arrangement of dampers [11]; however, optimal MR damper arrangement and their sensors as two discrete subjects have not received much attention yet [12–14].

Classical optimization methods are not compatible for solving complex engineering problems. The recent generation of the optimization algorithms is meta-heuristics, which are suggested to solve multi-objective engineering problems. A meta-heuristic algorithm consists of a group of search agents that study one possible region based on both randomization and some predefined rules [15]. These optimization algorithms are inspired by the natural behavior of animals in nature such as dolphins, etc. The dolphins transmit two intertwined ultrasound beams at different frequencies at different times during the process of echolocation. Scientists developed a mathematical formulation to successfully extract and read the overlapping signals. This discovery could lead to a sharper image quality on ultrasound technology [16]. The computational time of the control system should be minimized to eliminate the time delay effects. The Dolphin Echolocation (DE) algorithm demonstrated the fast and reliable optimization in comparison with other algorithms, such as genetic algorithm, particle swarm optimization, and ant colony optimization in several researches [17–20]. The DE optimization algorithm was proposed based on the process of foraging preys utilizing echolocation in dolphins and it is similar to discovering an optimal solution in a search space. Kaveh and Farhoudi idealized the DE for optimization algorithm [21].

Among several structural controllers provided so far, the Fuzzy Logic Controller (FLC) has obtained stable, reliable and appropriate semi-active control results in reducing the response of structures during severe earthquakes [22,23]. However, classical controllers require some pre-known and exact information about the specifications of a structural system whose mathematical matrix is to be prepared. Furthermore, a complex controller such as Linear Quadratic Gaussian (LQG) requires a solution to comprehensive constrained multi-objective optimization problems [24]. As a result, soft-computing techniques have been proposed to attenuate the complexity of obstacles including neural networks [25] and fuzzy logic [26]. Thereupon, recent studies have pursued adaptive controllers because they are more reliable and effective [27,28]. In this research, a Dolphin Echolocation-Fuzzy Logic Controller (DE-FLC) was proposed to combine the positive aspects of both methods.

To investigate the performance of structures during seismic motions, several analytical methods have been proposed, including static linear, linear dynamic dynamics, nonlinear static, and nonlinear dynamic methods. However, due to the shortcomings and limitations of static methods, they cannot be used in functional analysis. Furthermore, although dynamic methods enjoy greater suitability, they are very time-consuming and costly due to the large number of analyses. As a consequence, to improve the shortcomings of the previous seismic analysis methods, a new incremental dynamic method called Endurance Time Analysis (ETA) is proposed [29]. By applying a series of pre-designed accelerator increment functions, the seismic performance of the structure is examined. ETA provides an appropriate estimation of the structure's response to the intensity of different excitations based on the ASCE design spectrum. In comparison with other methods, this method reduces the number of required analyses to evaluate the structure, without heavy computational burden. Furthermore, compared to other linear and nonlinear methods, ETA unrestrictedly considered the behavioral complexities of the structure such as nonlinear behavior, effect of control

systems, etc. The ETA method exhibits appropriate efficiency in analysis of structures equipped with passive damper [30,31]. To the best of the author's knowledge, no research has not investigated the efficiency of ETA in the structural systems equipped with semi-active dampers, yet.

In traditional controllers, heavy computational burden is required in several seismic time history analyses. In this research, the utilization of ETA analysis is proposed to reduce the time and number of computational analysis requirements for designing semi-active controller systems. Furthermore, a DE-FLC is proposed to make use of the adaptability of a FLC simultaneously with the speed of DE optimization algorithm. An effective DE-FLC is utilized to enhance the efficiency of the MR damper and optimize its external energy consumption during seismic excitation. DE-FLC manages the MR damper output force by transmitting electrical input current. To identify the absolute velocity and the displacement of stories independently, separate sensors were determined. To this end, the DE-FLC calculates the inducement of electrical current to produce a magnetic field based on the displacement and the velocity of the floors. The excessive responses of an 11th-story building equipped with MR dampers were investigated in two cases of seven time-history analysis and six-generation Endurance Time (ET) functions. Simultaneously, the optimal arrangement and the number of sensors and dampers were determined through DE. The proposed DE-FLC controller exhibits its efficiency by reducing the excessive displacement under earthquake in comparison with the uncontrolled case and classical FLC. The results demonstrate that the sixth generation of ETA can simulate the results of several time history analyses well, without any computational burden.

2. The MR damper model description and simulation assumptions

The principal subject on the planning of a semi-active structural controller is considered in which the semi-active control strategy should be used. The time-delay effect leads to attenuation of the reliability of a structural controller. A semi-active controller, which reduces the analysis processing time and does not need any modification during the natural hazards, will have higher proficiency. FLC gathers these characteristics for the structural controller. By transmitting external voltage supply, the DE-FLC manages the mechanical behavior of the MR dampers. To enhance the efficiency of the controller, the location of sensors was determined without considering the arrangement of dampers. Moreover, to determine the external forces of damper, the input data of FLC were defined as absolute velocity and displacement of stories. Furthermore, more stories were involved in determining the damper forces. The semi-active controller should be optimized to minimize the control force of dampers and structural vibration magnitudes. For this purpose, the multi-objective optimization problem consists of three objective functions to be optimized. The arrangement of sensors and dampers is considered as a search space of the optimization process. For an optimal arrangement problem, the number of utilized sensors and MR dampers was considered as optimization constraints. The DE-FLC is utilized to solve the MR damper and sensor optimization problem. A state space should be utilized to simulate the displacement and velocity of MR damper over a wide range of loading situations. MR dampers consist of a semi-solid fluid, which transfers between two different chambers. A coil generates a magnetic field and modifies the characteristics of the MR fluid in the piston when electrical current is applied. The ability of MR fluids to modify from the free-flowing viscous fluids to semi-solids fluids in MR damper was utilized. Therefore, in a few milliseconds, MR damper has an adjustable control force when subjected to a magnetic field. Magneto-rheological fluid is able to respond to the applied magnetic field with a rapid modification by maintaining the reversibility of properties. Since 1996, 20 Ton MR dampers have been experimentally tested, designed, and utilized [24]. The equations of n-story structure responses could be defined via the following equations:

$$y(t)=C.Z(t)+D.u(t), \qquad \dot{Z}(t)=A.Z(t)+B.u(t), \quad (1)$$

where:

$$A=\begin{bmatrix} 0_{n\times n} & I_{n\times n} \\ -M_S^{-1}.K_S & -M_S^{-1}.C_d \end{bmatrix},$$

$$B=\begin{bmatrix} 0_{n\times n} & 0_{n\times n} \\ -I_{n\times n} & -M_S^{-1}.D_p \end{bmatrix},$$

$$C=\begin{bmatrix} I_{n\times n} & 0_{n\times n} \\ 0_{n\times n} & I_{n\times n} \\ -M_S^{-1}.K_S & -M_S^{-1}.C_d \end{bmatrix},$$

$$D=\begin{bmatrix} 0_{n\times n} & 0_{n\times n} \\ 0_{n\times n} & 0_{n\times n} \\ -I_{n\times n} & -M_S^{-1}.D_p \end{bmatrix},$$

$$Z(t)=\begin{bmatrix} X_{n\times 1} \\ \dot{X}_{n\times 1} \end{bmatrix}, \qquad u(t)=\begin{bmatrix} \ddot{X}_{g_{n\times 1}} \\ F(t)_{n\times 1} \end{bmatrix},$$

$$y(t)=\begin{bmatrix} X_{n\times 1} \\ \dot{X}_{n\times 1} \\ \ddot{X}_{n\times 1} \end{bmatrix}. \quad (2)$$

$\ddot{X}$, $\dot{X}$, and X in Eq. (2) are acceleration, velocity, and displacement vectors, respectively. The mass, stiffness,

and damping matrices are represented by M_S, K_S, and C_d, respectively. $u(t)$ is the output vector of the state space and $F(t)$ is the force of damper. D_p, $Z(t)$, and $y(t)$ demonstrate the damper placement, the state space, and output vector, respectively. In a close-loop process, the DE-FLC determines the control force of MR damper as a function of velocity and displacement responses of the building. Determining the optimal position and number of dampers and sensors is one of the main economic parameters in control strategy. For this purpose, the optimal number MR dampers were determined by DE in Section 5. In each time step, the following mechanical model of 20-Ton MR damper was employed to simulate the control force. The governing equations of MR dampers are described below:

$$\dot{y} = \frac{1}{C_0 + C_1}[\alpha \cdot Z + C_0 \cdot \dot{x} + k_0(x - y)],$$

$$f = C_1 \cdot \dot{y} + k_1 \cdot (x - x_0),$$

$$\dot{Z} = -\gamma\,|\dot{x} - \dot{y}|\,Z|Z|^{n-1} - \beta \cdot (\dot{x} - \dot{y})\,|Z|^n + A \cdot (\dot{x} - \dot{y})\,. \quad (3)$$

In the above equations, the parameters described as follows:

$$\alpha(i) = 16566 \cdot i^3 - 87071 \cdot i^2 + 168326 \cdot i + 15114,$$

$$C_0(i) = 437097 \cdot i^3 - 1545407 \cdot i^2 + 1641376 \cdot i + 457741,$$

$$C_1(i) = -9363108 \cdot i^3 + 5334183 \cdot i^2 + 48788640 \cdot i - 2791630. \quad (4)$$

In the above equations, x and y are the absolute and internal displacement of MR damper, respectively. $\alpha(i)$, $C_0(i)$, and $C_1(i)$ values of MR damper are experimentally determined and 'i' is the input current at each time interval. Other additional parameters are presumed constant as $n = 10$, $x_0 = 0.18$ m, $A = 2679$ m^{-1}, $k_1 = 617.31$ N/m, $k_0 = 37810$ N/m, γ and $\beta = 647.46$ m^{-1} to validate the experimental data. A first-order filter is also utilized to correctly adjust the dynamic mechanical model based on experimental data [32]:

$$H(S) = \frac{31.4}{S + 31.4}, \quad (5)$$

where S is the factor to correct the damper rod velocity which is estimated by a Kinematic Kalman Filter (KKF) from the relative displacement between base and first mass and from the absolute acceleration of the first mass [12–14]. The efficacy of time delay could be eliminated because the time delay is far from the first period of ordinary structures. The cumulative time delay associated with the closed-loop control and MR damper was less than 10 milli-second [33]. The electrical inducing current plays the main role to adjust the MR-damper external force during each time step. The input current is managed by FLC. The governing equations are expressed in Section 5. The configuration of MR damper is illustrated in Figure 1.

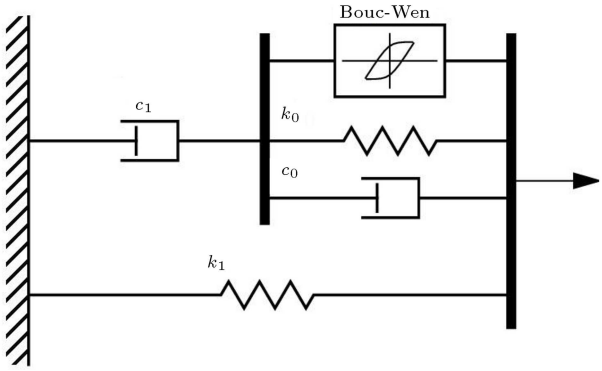

Figure 1. MR-damper mechanical model [12].

3. Fuzzy Logic Controller (FLC)

The classical controllers (such as H_2, LQR, etc.) rely heavily on the accuracy of modeling details as well as uncertainties and nonlinearities in magnitude of the loading and structural properties. The next generation of structural controllers could enhance the uncertainties and imprecision of modeling without having to solve any optimization problems. The proposed FLC includes four elements to resemble the logical reasoning of human brains. These elements are introduced as defuzzification interface, decision-making, rule base, and fuzzification interface. A DE-FLC controller was proposed to manage the uncertainty and imprecision, which was not considered in the controller design process. A closed-loop semi-active feedback controller was generated based on the following inference rules in Table 1.

Nine linguistic parameters were utilized as output and input fuzzy variables: ND (Negative-Displacement), NV (Negative-Velocity), ZD (Zero-Displacement), ZV (Zero-Velocity), PD (Positive-Displacement), PV (Positive-Velocity), L (Large), S (Small), and Z (Zero). To enhance the efficiency of input variables in FLC, an independent sensor for each MR damper is defined to transmit the velocity and displacement of sensors. The FLC is governing the MR damper by transmitting inducing current as

Table 1. The components of suggested FLC.

	NV	**ZV**	**PV**
ND	L	S	Z
ZD	S	Z	S
PD	Z	S	L

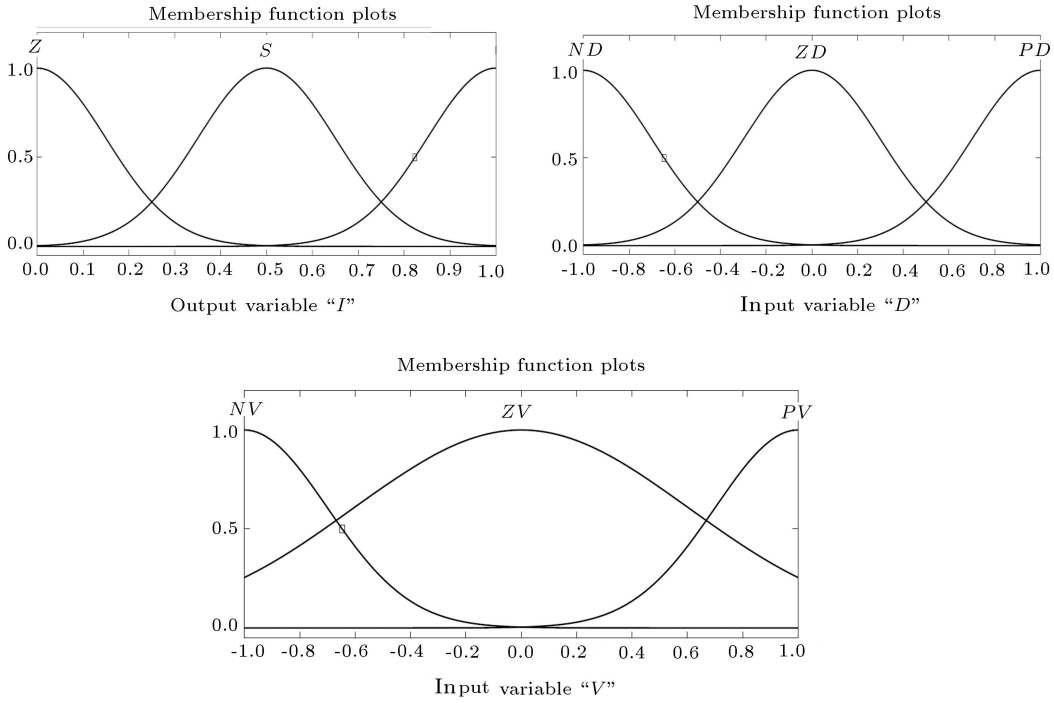

Figure 2. The input and output membership functions for the proposed FLC.

FLC output variable. In the proposed FLC, the range of membership functions for the output and input variables includes [0,1] and $[-1, 1]$, respectively. FLC decides that no significant control force is required if the velocity and the displacement of the MR-damper are non-directional. On the other hand, a major control force is mandatory if they are in the same direction. In the logical process of determining control output force, the gaussian curve membership functions were utilized. By utilizing the Mamdani-type fuzzy logic, the transmitted signal of sensors changes into linguistic-fuzzy values. Figure 2 illustrates the membership functions of output and input variables. The scale factor and quantification factor are determined by trial and error to improve the optimality of structural responses.

4. Dolphin echolocation optimization algorithm

The computational time of the control system should be minimized to eliminate the time delay effects. The DE algorithm demonstrated fast and reliable optimization in comparison with other algorithms [17–20]. Kaveh and Farhoudi introduced a novel optimization algorithm, which was inspired by the DE in nature [21]. The DE did not require extensive computational burden and parameter tuning. It could be widely utilized to solve various fields of optimization problems. Dolphins are capable to produce signals in the form of clicks with special frequencies. The part of sound-signal energy is reverberated to the dolphin when the signal collides an object. First off, dolphins search all around the search space to specify the prey. They regenerate sound signals sequentially to estimate the space between the objects by analyzing the time gap between echo and click. Moreover, the direction of object movements can be estimated by comparing the strength of the signal from two edges of the dolphin's head. Dolphin reiterates incrementally by generating clicks and obtaining echoes so that the target can be captured. It is possible that echolocation is familiar to optimization in some forms. The procedure of searching for preys by employing echolocation in dolphins is similar to concentrating on the optimal location in optimization problems. In the DE optimization algorithm, two phases could be defined. At the first phase, the DE searches all around the search space to accomplish a comprehensive search. This procedure is executed by tracking some random locations in the search space, and at the next phase, DE focuses on exploration around superior obtained results from the prior step. The metaheuristic values of DE parameters have been proposed by previous research studies [34]. The structure of the DE algorithm and the steps involved are illustrated in Figure 3.

Meta-heuristic algorithms are characterized by better proficiency in sorted design spaces. Therefore, before beginning the search procedure, the design search space needs to be sorted out. A curve should be determined based on the convergence factor during the optimization procedure. The adjustment of CF is

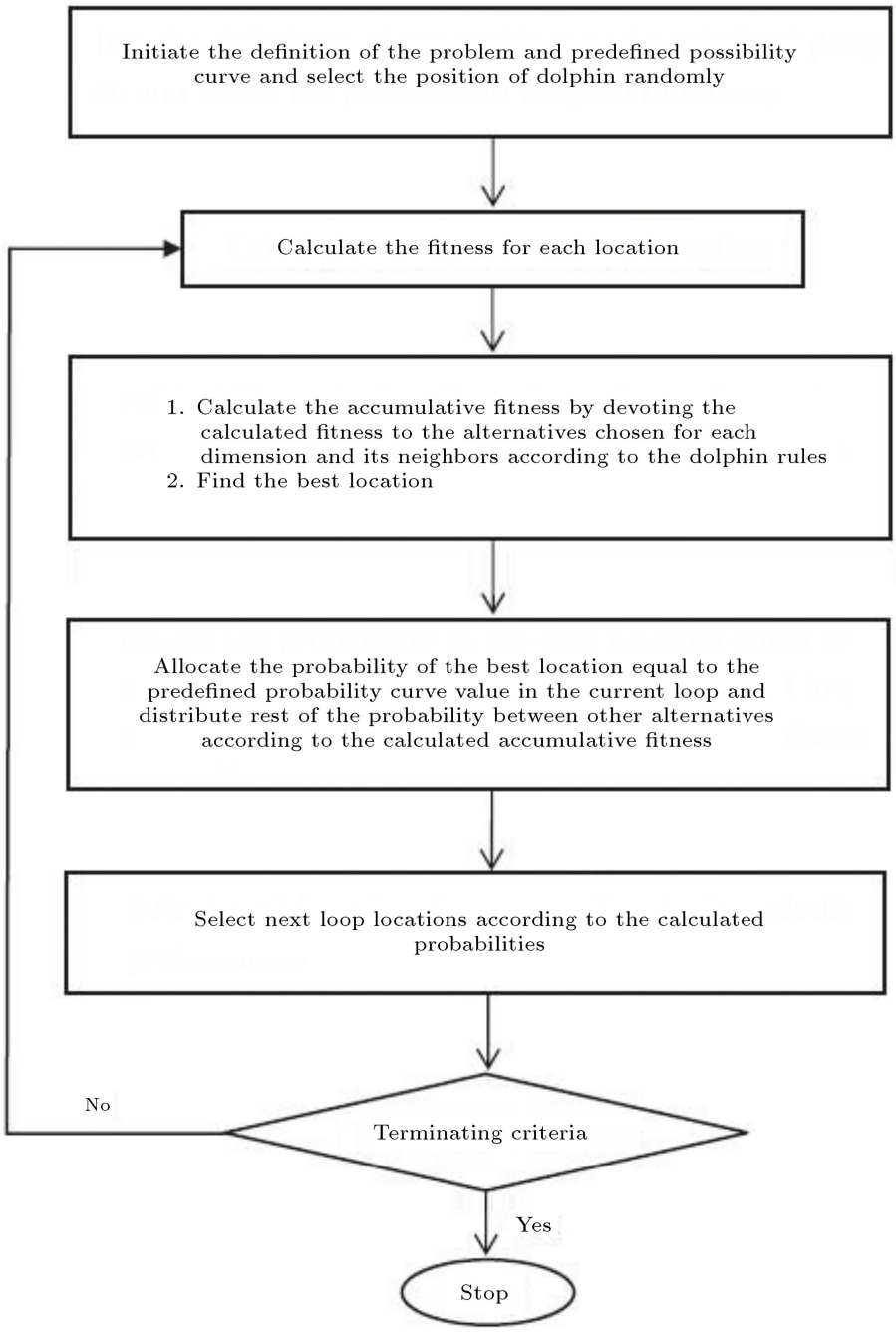

Figure 3. The structure of dolphin echolocation algorithm.

expressed as follows:

$$PP(Loop_i) = PP_1 + (1 - PP_1) \frac{Loop_i^{power} - 1}{(Loops\ number)^{power} - 1}. \quad (6)$$

In the above equation, PP, PP_1, $Loop_i$, $power$, and $Loops\ number$ are defined as probability, the convergence factor of the start loop, the number of the running loops, the degree of the curve, and number of loops in which the algorithm should converge to the optimal point, respectively. The solution of the traditional FLC is assumed to be one solution to reach the optimal value of MR damper inducing current.

The following DE algorithm procedure for discrete optimization should be employed to obtain an optimal location:

1. Spread NL placements for each dolphin in a random manner. This phase includes generating $L_{NL\times NV}$ matrix. The NV and NL are the number or dimension of each placement and number of dolphin's placements, respectively;

2. By using Eq. (1), compute the PP of the loop;
3. Compute the objective of each placement. Fitness functions should be specified such that better results get higher magnitudes based on Eq. (10);
4. Compute the accumulative objective function based on dolphin rules through the following process:
   (a) For $i = 1$ to the number of dolphin's placements;
   For $j = 1$ to the number of dimensions;
   For $k = -R_e$ to R_e;
   Determine the location of $L(i, j)$ in the jth column of the alternative matrix as A.

$$AF_{(A+k)j} = \frac{1}{R_e} \times (R_e - |k|) \times Fitness(i) + AF_{(A+k)j}. \quad (7)$$

   End
   End
   End
   In the above equation, $AF_{(A+k)j}$ is the accumulative objective function of the $(A + k)$th alternative (numbering of the alternatives is identical to the ordering of the Alternative matrix) to be elected for the jth variable. Furthermore, R_e is the efficient radius of the search area in which the accumulative fitness of the alternative A's neighbors was impressed from its fitness values. The search radius is recommended to be less than 1/4 of the search space. Moreover, *Fitness(i)* is the fitness value in the placement of i. Of note, for the alternatives near the sides (where $A + k$ was not valid; $A + k < 0$ or $A + k > L_{Aj}$), the AF was computed using reflective specifications. Thus, if the distance of an alternative to the side is not more than R_e, the same alternative presumably exists where the mentioned alternative is observed if a mirror is positioned on the side.
   (b) In order to expand equal opportunities in the search space, a small value was randomly added to all the arrays as $AF = AF + \varepsilon$. Based on the way the fitness was determined, ε should be determined. It should be less than the minimum value obtained for the fitness.
   (c) Determine the optimal placement of this loop and name it "the optimum placement". Determine the alternatives assigned to the variables of the optimum location and let their AF be zero.
5. For variable j ($j = 1$ to NV), compute the probability of determining alternative i ($i = 1$ to LA_j) as follows:

$$P_{ij} = \frac{AF_{ij}}{\sum_{i=1}^{LA_j} AF_{ij}}. \quad (8)$$

6. Assign a probability equal to PP to all the alternatives elected for all variables of the optimum placement and devote the rest of the probabilities to the other alternatives as follows:
   for $j = 1$ to Number of variables
      for $i = 1$ to Number of alternatives
         if $i =$ The best location (j) of dolphins
            $PP = P_{ij}$
         else

$$PP = (1 - PP).P_{ij}, \quad (9)$$

         end
      end
   end

Compute the next phase locations based on the possibility assigned to each alternative. Until loops number is determined, steps 2 to 6 should be reiterated. To ensure better diversity, the proposed procedure prepares opportunities for the agents to move all over the search space. The termination criterion is supposed to be the maximum number of iterations limited to 60.

Finally, the population size, N, is specified to be 70. These selections are based on the trial-and-error process to optimize the most appropriate convergence accuracy and speed in the DE algorithm. For each time window, the fitness function is determined as follows:

$$J_1 = \frac{\sum^{n} RMS(x_{FLC})}{\sum^{n} RMS(x_{POFF})}, \qquad J_2 = \frac{\sum^{n} RMS(d_{FLC})}{\sum^{n} RMS(d_{POFF})},$$

$$J_3 = \frac{\sum^{n} RMS(\ddot{x}_{FLC})}{\sum^{n} RMS(\ddot{x}_{P_{OFF}})}. \quad (10)$$

In the above equation, RMS is the abbreviation of root mean square. Herein, d, x, and $\ddot{x}$ are the inter-story drift, absolute displacement, and acceleration of the floors, respectively. The superscript P_{OFF} indicates the case where the dampers operate in the passive-off mode and MR damper acts as a passive viscous device. The final case is the FLC. In this case, the operational range of MR dampers is determined to be in the range of 0 to 1 V.

5. Numerical simulations and results of DE-FLC

Seismic time history analyses require heavy computational burden. In this research, the utilization of ETA analysis is proposed to reduce the time and number of analysis requirements in designing a semi-active

controller system. For this purpose, the numerical results are achieved in MATLAB software using the state-space model.

5.1. Optimal sensor and damper placement by using DE algorithm and FLC controller

In this research, an eleven-story concrete moment frame is utilized to illustrate the efficiency of the DE-FLC. The modeling assumptions are as follows:

1. Each floor is assumed to be a rigid diaphragm;
2. The mass of each class is considered as a concentrated mass;
3. The behavior of materials in the linear range.

The structural specifications of the concrete moment frame including the mass and stiffness of each floor are given in Table 2 and Figure 4. The damping matrix is determined by combining the mass and stiffness of the structural system. The coefficients a_0, b_0 are obtained for the first and second modes of the structural system and the damping coefficient $\xi_i = \xi_j$ is considered 5% in Eq. (12).

$$[C] = a_0[M] + b_0[K], \tag{11}$$

$$b_0 = \xi_j \times \frac{2}{\omega_i + \omega_j}, \qquad a_0 = \xi_i \times \frac{2\omega_i \times \omega_j}{\omega_i + \omega_j}. \tag{12}$$

In the first step, to illustrate the efficiency of the proposed DE-FLC in ETA method, the optimal number and location of damper and their sensors should be determined. For this purpose, three fitness functions were utilized in Eq. (10). The economic considerations should be utilized to determine the number of dampers, because a larger number of dampers lead to more attenuated seismic responses of buildings. Therefore, a Penalty Function (PF) should be utilized to achieve

Table 2. The mass and stiffness of concrete moment frame.

Number of stories	Mass (Ton)	Stiffness (kN/m)
1	215	4680
2	201	4760
3	201	4680
4	200	4500
5	201	4500
6	201	4500
7	201	4500
8	203	4370
9	203	4370
10	203	4370
11	176	3120

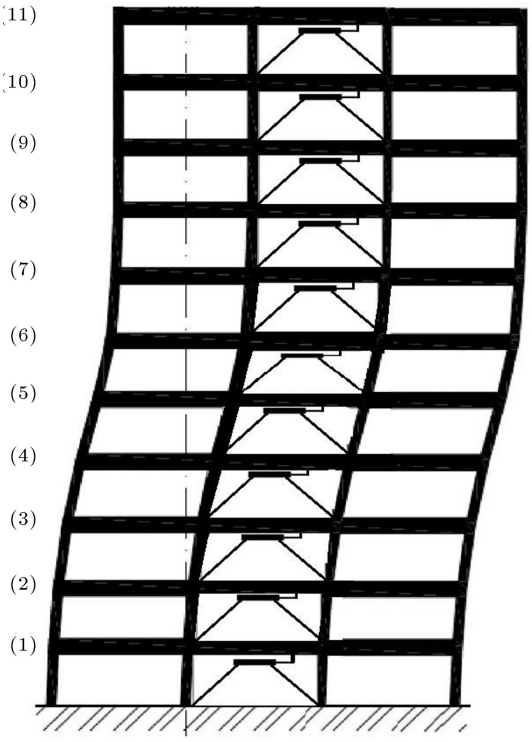

Figure 4. 11th story benchmark building with possible MR damper location.

the optimum number of sensors and dampers. The following PF was utilized:

$$PF = (2 \times J_1 + 1 \times J_2 + 0.8 \times J_3) \times (1 + ND \times 0.07), \tag{13}$$

where J_1, J_2, J_3, and ND are three objective functions and number of dampers, respectively. A forward-directivity near-fault El-Centro acceleration was utilized to excite the benchmark structure. The DE determines the number and arrangement of the dampers and sensors to minimize the structural responses by utilizing PF, J_1, J_2, and J_3. Finally, to optimize the optimal placement and number, the structural responses were compared with the passive-off and passive-on cases during time-history analysis. The matrix of DE particles includes the number and the arrangement of the MR dampers and their sensors. The propriety of the DE population moderately is enhanced with respect to Eq. (13). To enhance the probability of determining the optimum global solution in meta-heuristic algorithms, five independent DE algorithms were initially simultaneously. The local and global best parameters were updated in each 5 iterations between these optimization algorithms. By utilizing 60 initial particles, DE could determine the optimal solution after the 19th iteration. The optimal solution is determined as follows:

$$D_p = \begin{bmatrix} 0 & 0 & 2 & 1 & 2 & 2 & 0 & 1 & 2 & 2 & 2 \end{bmatrix},$$

$$S_p = \begin{bmatrix} - & - & 4 & 6 & 7 & 7 & - & 8 & 10 & 10 & 11 \end{bmatrix}, \tag{14}$$

Table 3. The absolute maximum results of 11th-story structural system [33] in Elcentro earthquake.

The case of structural responses	Uncontrolled structure	Controlled structure			
		P_{OFF}	P_{ON}	Clipped-optimal controller	DE-FLC
11th floor max drift (cm)	0.114	0.092	0.078	0.081	0.061
11th floor maximum displacement (cm)	0.41	0.33	0.28	0.29	0.24

where D_p and S_p are the sensor and damper arrangement vectors, respectively. The DE illustrates that the optimum number of MR dampers is fourteen. Two 200 kN MR dampers should be placed on the 3rd, 5th, 6th, 9th, 10th, and 11th stories and one damper is required to be on the 4th and 8th stories. Also, their sensors should be placed, as shown in S_p vector, on the stories of the building. An independent DE-FLC is utilized in each story where the sensor is installed. Based on the displacement and the velocity transmitted from sensors, DE-FLC decides to transmit the inducing current to generate the magnetic field. The viscosity of MR fluid rapidly changes to adjust the required stiffness and damping coefficient in MR damper. Table 3 illustrates the displacement and drift responses of DE-FLC in comparison with other traditional control cases. By utilizing DE-FLC, Significant reductions were obtained in J_1 and J_2, which correspond to the RMS of the absolute acceleration, inter-story drifts, and displacement responses. Based on the impact factors assumed in Eq. (10), J_3 experienced less reduction which corresponds to the RMS of absolute acceleration in stories. Overall, the DE-FLC efficiency was superior to the passive-on control case with respect to all control cases except the peak absolute acceleration. To indicate the proficiency of DE-FLC more precisely, the controlled responses were compared with passive and semi-active controlled cases. In the passive case indicated by 'P_{OFF}', no inducing current is transmitted during seismic excitation. In another passive controller indicated by 'P_{ON}', the inducing current was kept constant at the maximum current-inducing value (3.0 A). Furthermore, the efficiency of the DE-FLC is compared with the previously studied clipped-optimal controller [33].

Results demonstrate that DE-FLC could outstandingly increase the performance of a semi-active controlled structure. The P_{OFF} controller decreases the peak displacement of the top floor by 19% of the uncontrolled responses, the P_{ON} controller demonstrates 32% reduction, the clipped-optimal controller exhibits 29% reduction, and the DE-FLC attenuates the responses up to 46%. Despite the reduction of displacement in other controllers, the DE-FLC exhibits superior performance in reducing the undesired structural vibration with the same number of dampers and sensors.

5.2. Preparation of seismic excitation in accordance with ASCE regulations

In this research, ASCE41_06 regulations, which have been presented by ASCE Institute under the title of seismic improvement of buildings, were employed [35]. In this regulation, the design of the structure is based on seismic performance, and it includes five non-structural performance levels, which are named risk levels. Risk levels include (a) BSE-2 risk level representing the most likely earthquake with a probability of occurrence of 2% in 50 years or 2475 years return period and (b) BSE-1 risk level representing 10% probability of earthquake occurrence in 50 years or 475 years return period. Furthermore, two subhazard levels include 20%/50 and 50%/50 years, with 20% and 50% probabilities of occurrence in 50 years, respectively. According to the rules of this regulation, seven series of accelerometers can be used to analyze the time history and the average response values can be used to evaluate the performance of the structure. In this research, seven earthquake records are selected from the FEMA 440 proposed records for soil of type C [36]. After determining the initial coefficients, seven accelerometers should be scaled. The accelerometers should be in the range of 0.2 T to 1.5 T above the spectrum of each level of ASCE41 regulations, where T is the period of the uncontrolled building. This scale factor was based on the main period of the uncontrolled structure. Table 4 illustrates the specifications of seven selective accelerometers and primary scale coefficients under a set called GMI, and Table 5 shows the scale coefficients for an eleven-story structure with the main period time of 0.975 second for different risk levels.

5.3. ET method

In the ET method, choosing a proper type of acceleration time ET functions is essential to obtain the consistency and accuracy of the results. Therefore, to estimate the nonlinear responses of seven time-history analysis for the structure equipped with semi-active MR damper controller, the sixth generation of ETA20e01-03 functions was used. The features of this series of generation of ET functions included good accuracy in nonlinear analyses as well as covering long periods [37]. The correct interpretation of the responses of the analysis of durability time and the time mapping in its functions fully depend on the seismic

Table 4. Specifications of seven selective accelerometers based on FEMA-440.

Date of occurrence	Station of earthquakes	Magnitude (Ms)	Station number	Component (deg)	PGA (cm/s^2)	Scale factor
6/28/1992	Landers	7.5	12149	0	167/5	3.64
10/17/1989	Loma Prieta	7.1	58065	0	494/5	1.44
1/17/1994	Northridge	6.8	24278	360	504/2	1.07
4/24/1984	Morgan Hill	6.1	57383	90	280/4	1.84
10/17/1989	Loma Prieta	7.1	47006	67	349/1	2.20
10/17/1989	Loma Prieta	7.1	58135	360	433/1	2.29
10/17/1989	Loma Prieta	7.1	1652	270	239/4	2.61

Table 5. Scale factor of building based on ASCE41-06

Risk level	Scale factor
BSE-1	0.965
BSE-2	1.375
50%/50 years	0.488

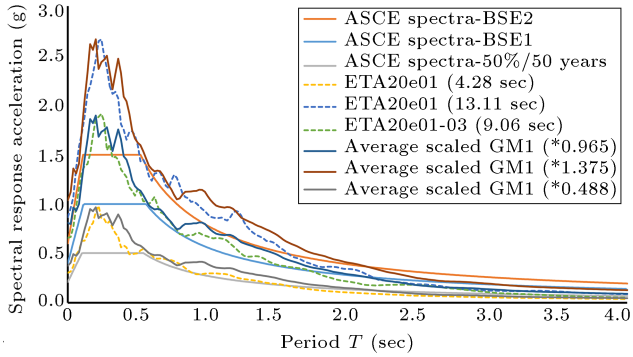

Figure 5. Rules spectrum, scale measurement scale (GMI), and e-series levels at different risk levels.

motion intensity. In other words, it is sufficient that the spectrum of functions of the acceleration time of the resistance at a given time (target time) corresponds to one of the design spectra or the average spectrum of earthquake records or the spectrum of responses due to seismic risk analysis. As shown in Figure 5, to determine the target time series E, an attempt was made to use the mean spectrum of ASCE41-17 matching of these functions with the mean range of the set (GMI), which is shown in Table 6. By using the new approach for ETA method [38,39], the time-domain spectral matching algorithm was modified and utilized in several time durations. Furthermore, the matching precision is significantly enhanced and the computation time is attenuated.

5.4. Evaluation of time endurance curve by using DE-FLC

After the development of the DE-FLC, the performance of the proposed controller in reducing structural seismic responses is investigated on the ET curves.

Table 6. Target time function of acceleration time function at ASCE41-17 risk levels.

Risk levels of ASCE41-17	Mean Target time (S) of ETA20e01-03
BSE-2	13.11
BSE-1	9.06
50%/50 years	4.28

The structure is examined by considering the relative displacement of floors as well as the maximum displacement of the last floor in case of before and after the rehabilitation by MR dampers. Figure 6 illustrates the maximum displacement of the top floor under the 6th generation of ETA20e01, ETA20e-02, and ETA20e-03 accelerations. The results demonstrate that the optimal placement of MR damper by using DE-FLC controller reduced the maximum displacement of the top floor by 30% to 40%. Figure 7 shows the maximum displacement of the top floor under Morgan Hill, Landers, and Northridge seismic excitations, respectively. In this case, the mean of ETAs results can be used to simulate the displacement of the top story of the structure under the mean of seven real seismic excitations.

To investigate risk levels more precisely, the results of ETA method are usually provided with the help of an incremental curve. In this curve, the horizontal and vertical axes are the time and maximum drift response of the structure under different demand parameters, respectively. In this research, these curves are also smoothed using the moving average method to eliminate stagnation. In Figure 8, the ETA curve for the structural system is drawn in two cases of uncontrolled and DE-FLC controlled. The relative displacement of the floors is illustrated in all cases and then, the drift results are compared with the allowable limits of the ASCE regulations. According to the ASCE41-17 regulations, the allowable values of relative displacement of the structural system are considered to be 5% for CP level as well as 2.5% and 0.7% for LS and IO levels, respectively. Therefore, the structure must

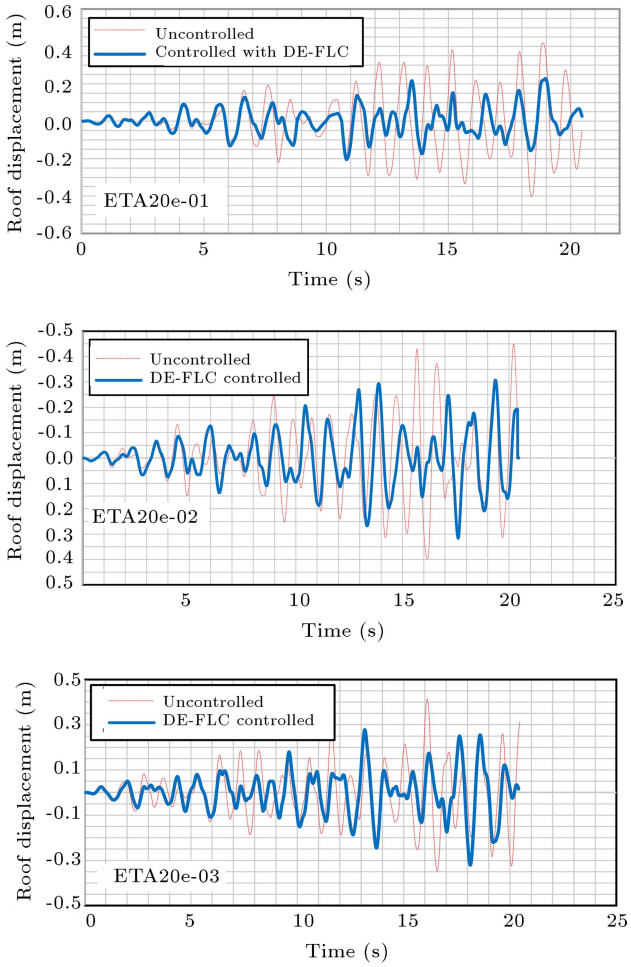

Figure 6. Displacement of top story in case of uncontrolled and DE-FLC controlled under ETA20e02 and ETA20e03.

satisfy the Collapse Prevention at the BSE-2 risk level and the Life Safety level at the BSE-1 risk level [35]. Based on Figure 8, the structure performed poorly without any damper, but the addition of MR dampers with DE-FLC controller could change the performance of the structure at ASCE levels.

By using DE-FLC controller, the ET of the structure increased from 6.31 (s) to 9.56 (s) in ETA curves. In other words, the rehabilitated structure could resist against BSE-2 seismic excitation. Figures 9 and 10 demonstrate a comparison between the relative displacement of the floors under the acceleration functions of ETA20e01-03 and GMI excitation series. It can be observed that the relative displacement of the building in general has followed a downward trend, and the same results are observed in the study of ETA functions without heavy nonlinear complex time history analysis. Thus, it can be said that the mean of ETA functions has provided a good prediction of the behavior of the structure under the mean of several earthquake records.

The relative displacement of the floors in uncon-

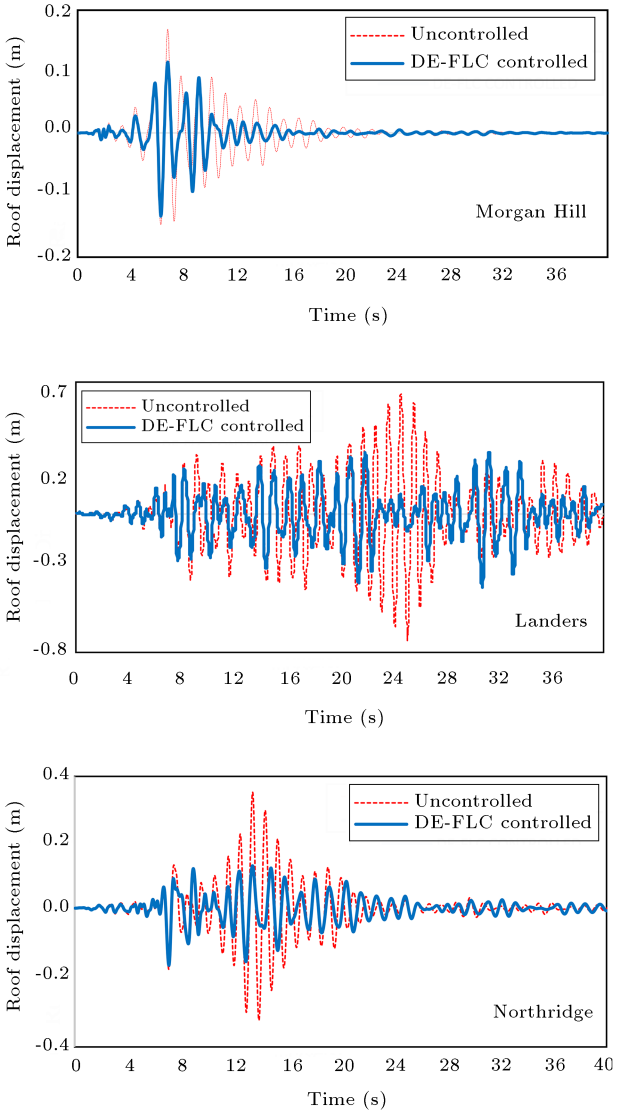

Figure 7. Displacement of top story in uncontrolled and controlled cases with DE-FLC controlled under the Morgan Hill, Landers, and Northridge records.

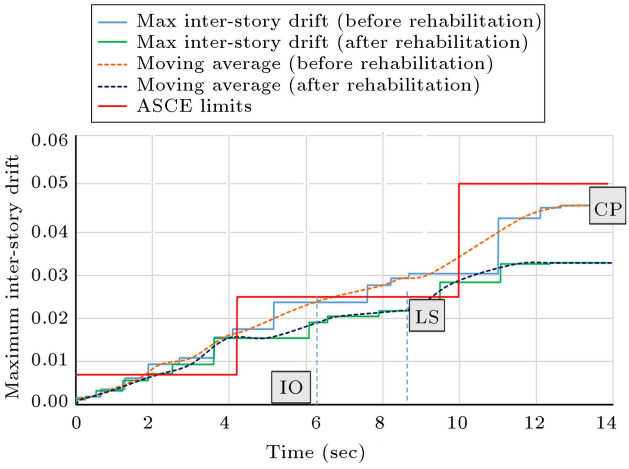

Figure 8. Time endurance curves of structures in uncontrolled and controlled cases with DE-FLC.

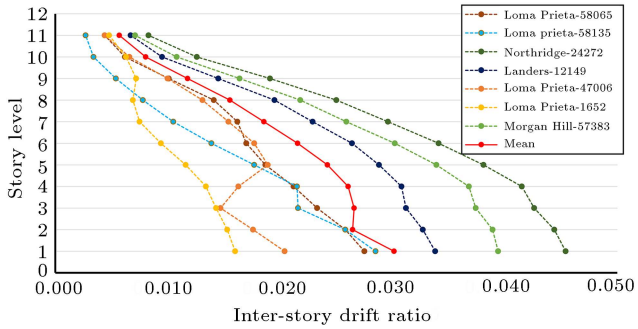

Figure 9. Inter-story drift ratio under GMI seismic records.

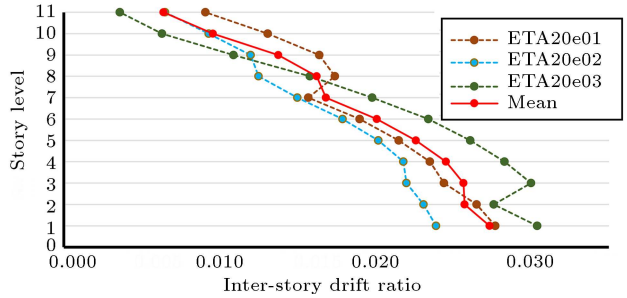

Figure 10. Inter-story drift ratio under ETA records.

trolled and controlled cases with DE_FLC for the BSE-2, BSE-1 and 50%/50-year hazard levels is investigated in Figures 11 and 12. To evaluate the performance of the DE-FLC in attenuating the seismic response of the structure, the ETA curves were compared with seven GMI records. As can be seen, the structure had seismic responses close to the limits of the ASCE regulations and even beyond before the rehabilitation with DE-FLC. The DE-FLC could efficiently improve the seismic performance of the structure to the allowable ASCE drift ratio by decreasing the responses. At the BSE-1 hazard level, the drift ratio of the building is reduced by 24%, indicating the proper efficiency of DE-FLC. Furthermore, it can be seen that the ETA curve predicts the trend of displacement the same as structural responses of the average of seven GMI series records.

As demonstrated by the results, the ETA curves could predict different levels of structural seismic demands. Table 7 shows the precision of ETA curves in comparison with seven seismic excitations of GMI records.

By and large, the simulation results demonstrate that the sixth generation of ETAs can simulate the vibration results of time history analyses well without heavy constrained computational burden. The mean of error percentages for drift ratio in case of ETA analysis is 8%, 8%, and 7% for uncontrolled cases and 12%, 8%, and 8% for controlled cases, respectively, at different seismic risk levels. The error percentages for ETA analysis in comparison with the mean of several time

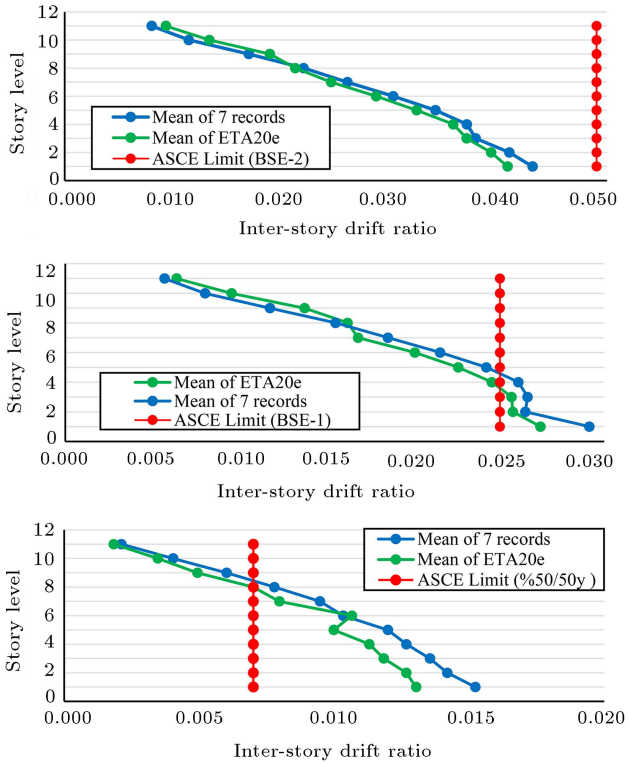

Figure 11. Inter-story drift ratio under the mean of ETA and GMI records in the uncontrolled case.

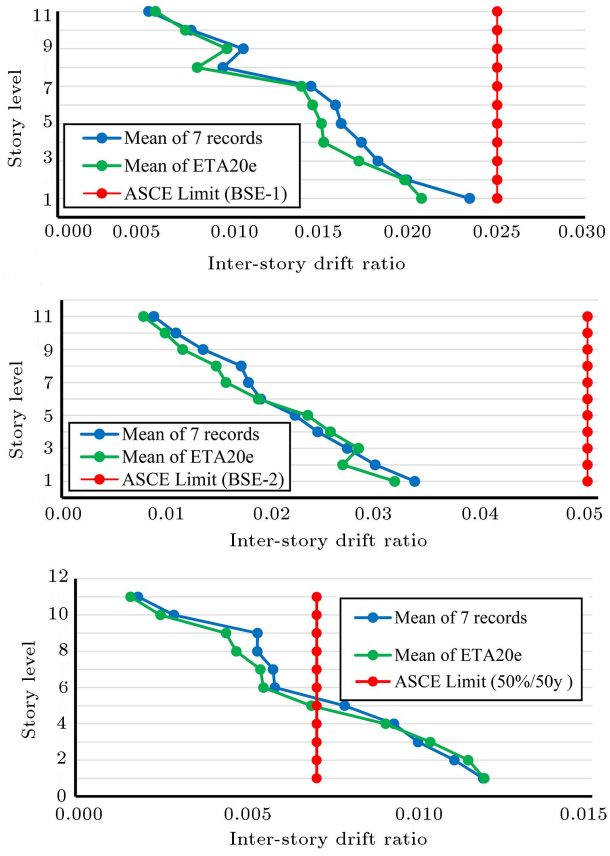

Figure 12. Inter-story drift ratio under the mean of ETA and GMI records in the controlled case.

Table 7. Error percentages of drift ratio in case of ETA analysis in comparison with time history analysis.

Seismic risk level	BSE-2		BSE-1		50%/50 years	
Story	Simulation error percentage (%)					
	Uncontrolled	DE-FLC controlled	Uncontrolled	DE-FLC controlled	Uncontrolled	DE-FLC controlled
1	0.3	13.4	9.3	11.6	5.35	5.6
2	3.5	10.7	2.7	0.6	4.1	10.3
3	3.5	12.6	3.5	5.9	2.1	3.8
4	2.6	10.8	5.8	12.4	3.3	4.7
5	12.4	14.7	6.7	7	5.1	5.1
6	5.7	3	6.8	8.2	5.2	1.3
7	6.5	13.9	9.3	3.8	5.7	12
8	11.6	10.1	4.3	14.3	3.5	13.8
9	17.4	18	14.1	8.8	10.2	14.4
10	13.7	13.9	14.7	4.2	14.1	9.6
11	11.7	13.3	10.9	7.1	14	11.1

history analyses were less than 15% at BSE-1 and BSE-2 seismic risk levels. In comparison with the risk level of 50% in 50 years, the error in the worst case reached 17.4% while the mean of the errors associated with all the stories were acceptable.

6. Conclusions

A novel dolphin echolocation was utilized to optimize the sensor and MR damper arrangement for the attenuation of building responses subjected to GMI series and the 6th generation of Endurance Time Analysis (ETA) records. Furthermore, Dolphin Echolocation-Fazzy Logic Controller (DE-FLC) was introduced to manage the inducing current of the MR-dampers in a semi-active controlled structure. Numerical results and simulation illustrated the efficiency of DE-FLC. The DE_FLC managed to reduce the structural responses up to 30–40% in comparison with the uncontrolled case. The simulation efforts demonstrated that the modified DE-FLC controller was a practicable technique and superior to the clipped optimal control.

Moreover, numerical studies have been done to demonstrate the ability of the sixth generation of ETA to simulate the responses of controlled structure as well as time history analyses without any heavy constrained computational burden. The following results are given in brief:

1. The DE_FLC could attenuate the maximum displacement of the top floor and drift by about 30% and 40%. It also reduced the relative displacement between the floors and the maximum allowable limits set in the ASCE regulations were observed;
2. The target time of ETA curves increased from 6.31 seconds to 9.31 by using DE-FLC controller, which indicated the increase in structural durability time;
3. The results demonstrate that durability method had the ability to predict the behavior of semi-active controlled structures with a minimum number of analyses and appropriate error percentage. The ETA predic2ted the drift trend in stories and risk levels with a reasonable approximate;
4. Based on the comparison of the trend of changes in structural response diagrams under series E of ETA and seven selected GMI accelerometers, it can be concluded that the responses resulting from the ETA provide an acceptable estimate of the actual acceleration responses and have a maximum error of less than 18%.

References

1. Aghajanian, S., Baghi, H., Amini, F., et al. "Optimal control of steel structures by improved particle swarm", *International Journal of Steel Structures*, **14**(2), pp. 223–230 (2014). https://doi.org/10.1007/s13296-014-2003-3
2. Amezquita-Sanchez, J.P., Valtierra-Rodriguez, M., Aldwaik, M., et al. "Neurocomputing in civil infrastructure", *Scientia Iranica*, **23**(6), pp. 2417–2428 (2014). https://doi.org/10.24200/SCI.2016.2301
3. Fisco, N.R. and Adeli, H. "Smart structures: Part I–Active and semi-active control", *Scientia Iranica*, **18**(3), pp. 275–284 (2011). https://doi.org/10.1016/j.scient.2011.05.034
4. Zabihi-Samani, M. and Amini, F. "A cuckoo search controller for seismic control of a benchmark tall building", *Journal of Vibroengineering*, **17**(3), pp. 1382–1400 (2015).
5. Zabihi-Samani, M. and Ghanooni-Bagha, M. "Optimal semi-active structural control with a wavelet-based cuckoo-search fuzzy logic controller", *Iranian Journal*

of Science and Technology, Transactions of Civil Engineering, pp. 619–634, **43**(1), (2018). https://doi.org/10.1007/s40996-018-0206-0

6. Bigonah, M., Soltani, H., Zabihi-Samani, M., et al. "Performance evaluation on effects of all types of infill against the progressive collapse of reinforced concrete frames", *Asian Journal of Civil Engineering*, **21**(3), pp. 395–409 (2020). https://doi.org/10.1007/s42107-019-00208-z
7. Honarvar, H., Shayanfar, M.A., Babakhani, B., et al. "Numerical analysis of steel-concrete composite beam with blind bolt under simultaneous flexural and torsional loading", *Civil Engineering Infrastructures Journal*, **53**(2), pp. 379–393 (2020). https://doi.org/10.22059/ceij.2020.287376.1606
8. Sodeyama, H., Suzuki, K., and Sunakoda, K. "Development of large capacity semi-active seismic damper using magneto-rheological fluid", *Journal of Pressure Vessel Technology*, **126**(1), pp. 105–109 (2004). https://doi.org/10.1115/1.1634587
9. Spencer, B.F., Dyke, S.J., Sain, M.K., et al. "Phenomenological model for magnetorheological dampers", *Journal of Engineering Mechanics*, **123**(3), pp. 230–238 (1997). https://doi.org/10.1061/(ASCE)0733-9399(1997)123:3(230)
10. Azimi, M., Rasoulnia, A., Lin, Z., et al. "Improved semi-active control algorithm for hydraulic damper-based braced buildings", *Structural Control and Health Monitoring*, **24**(11), e1991 (2017). https://doi.org/10.1002/stc.1991
11. Zabihi-Samani, M. "Design of optimal slit steel damper under cyclic loading for special moment frame by cuckoo search, *International Journal of Steel Structures*, **19**(4), pp. 1260–1271 (2019). https://doi.org/10.1007/s13296-019-00206-6
12. Vaishnav, S., Paul, J., and Deivanathan, R. "Model development and simulation of vehicle suspension system with magneto-rheological damper", *IOP Conference Series: Earth and Environmental Science*, **850**(1), 012035 (2021). https://doi.org/10.1088/1755-1315/850/1/012035
13. Li, G. and Yang, Z.-B. "Modelling and analysis of a magnetorheological damper with nonmagnetized passages in piston and minor losses", *Shock and Vibration*, **2020**, 2052140 (2020). https://doi.org/10.1155/2020/2052140
14. Zhang, S., Shi, W., and Chen, Z. "Modeling and parameter identification of MR damper considering excitation characteristics and current", *Shock and Vibration*, **2021**, 6691650 (2021). https://doi.org/10.1155/2021/6691650
15. Sabbagh-Yazdi, S.R., Farhoud, A., and Zabihi-Samani, M. "Transient Galerkin finite volume solution of dynamic stress intensity factors", *Asian Journal of Civil Engineering*, **20**(3), pp. 371–381 (2019). https://doi.org/10.1007/s42107-018-00111-z
16. Thomas, J., Moss, C., and Vater, A. "Echolocation in bats and dolphins", *Bibliovault OAI Repository*, the University of Chicago Press (2007).
17. Saedi Daryan, A., Salari, M., Farhoudi, N., et al. "Seismic design optimization of steel frames with steel shear wall system using modified dolphin algorithm", *International Journal of Steel Structures*, **21**, pp. 771–786 (2021). https://doi.org/10.1007/s13296-021-00472-3
18. Dehghani, M., Mashayekhi, M., and Sharifi, M. "An efficient imperialist competitive algorithm with likelihood assimilation for topology, shape and sizing optimization of truss structures", *Applied Mathematical Modelling*, **93**, pp. 1–27 (2021). https://doi.org/10.1016/j.apm.2020.11.044
19. Palizi, S. and Saedi Daryan, A. "Plastic analysis of braced frames by application of metaheuristic optimization algorithms", *International Journal of Steel Structures*, **20**(4), pp. 1135–1150 (2020). https://doi.org/10.1007/s13296-020-00347-z
20. Wei, C., Hoffmann-Kuhnt, M., Au, W.W.L., et al. "Possible limitations of dolphin echolocation: a simulation study based on a cross-modal matching experiment", *Sci. Rep.*, **11**(1), pp. 66–89 (2021). https://doi.org/10.1038/s41598-021-85063-2
21. Kaveh, A. and Farhoudi, N. "A new optimization method: Dolphin echolocation", *Advances in Engineering Software*, **59**, pp. 53–70 (2013). https://doi.org/10.1016/j.advengsoft.2013.03.004
22. Basu, B. and Nagarajaiah, S. "A wavelet-based time-varying adaptive LQR algorithm for structural control", *Engineering Structures*, **30**(9), pp. 2470–2477 (2008). https://doi.org/10.1016/j.engstruct.2008.01.011
23. Soto, M.G. and Adeli, H. "Placement of control devices for passive, semi-active, and active vibration control of structures", *Scientia Iranica*, **20**(6), pp. 1567–1578 (2013).
24. Yang, G., Spencer, B.F., Carlson, J.D., et al. "Large-scale MR fluid dampers: modeling and dynamic performance considerations", *Engineering Structures*, **24**(3), pp. 309–323 (2002). https://doi.org/10.1016/S0141-0296(01)00097-9
25. Nomura, Y., Furuta, H., and Hirokane, M. "An integrated fuzzy control system for structural vibration", *Computer-Aided Civil and Infrastructure Engineering*, **22**(4), pp. 306–316 (2007). https://doi.org/10.1111/j.1467-8667.2007.00487.x
26. MohsenAli Shayanfar, M.B., Sobhanim, D., and Zabihi-Samani, M. "The effectiveness investigation of new retrofitting techniques for RC frame against progressive collapse", *Civil Engineering Journal*, **4**(9), pp. 2132–2142 (2018). https://doi.org/10.28991/cej-03091145
27. Ostadali-Makhmalbaf, M., Tutunchian, M., and Zabihi-Samani, M. "Optimized fuzzy logic controller for semi-active control of buildings using particle

swarm optimization", *Advanced Material Research*, **2505**(9), pp. 255–260 (2011). https://doi.org/10.4028/www.scientific.net/AMR.255-260.2505

28. Raji, F. and Naeiji, A. "Performance of concrete MRF at near-field earthquakes compared to far-field earthquakes", *Civil Engineering Journal*, **5**(4), pp. 759–766 (2019). https://doi.org/10.28991/cej-2019-03091285
29. Estekanchi, H., Mashayekhi, M., Vafai, H., et al. "A state-of-knowledge review on the Endurance Time Method", *Structures*, **27**(9), pp. 2288–2299 (2020). https://doi.org/10.1016/j.istruc.2020.07.062
30. Rezaei, M., Ranjbar Karkanaki, A., and Zabihi-Samani, M. "Experimental investigation of deep beams containing high-performance fiber-reinforced cementitious composite", *Iranian Journal of Science and Technology, Transactions of Civil Engineering*, **46**(1), pp. 55–65 (2022). https://doi.org/10.1007/s40996-021-00653-4
31. Shirkhani, A., Mualla, I., Shabakhty, N., et al. "Behavior of steel frames with rotational friction dampers by endurance time method", *Journal of Constructional Steel Research*, **107**(5), pp. 211–222 (2015). https://doi.org/10.1016/j.jcsr.2015.01.016
32. Aggumus, H. and Cetin, S. "Experimental investigation of semiactive robust control for structures with magnetorheological dampers", *Journal of Low Frequency Noise, Vibration and Active Control*, **37**(2), pp. 216–234 (2018). https://doi.org/10.1177/0263092317711985
33. Xue, X., Sun, Q., Zhang, L., et al. "Semi-active control strategy using genetic algorithm for seismically excited structure combined with MR damper", *Journal of Intelligent Material Systems and Structures*, **22**(3), pp. 291–302 (2011). https://doi.org/10.1177/1045389X11399661
34. Gholizadeh, S. and Poorhoseini, H. "Seismic layout optimization of steel braced frames by an improved dolphin echolocation algorithm", *Structural and Multidisciplinary Optimization*, **54**(4), pp. 1011–1029 (2016). https://doi.org/10.3311/PPci.8155
35. American Society of Civil Engineers "Seismic evaluation and retrofit of existing buildings", *Seismic Evaluation and Retrofit of Existing Buildings*, ASCE/SEI 41–13 (2014). https://doi.org/10.1061/9780784412855
36. Khoshnoudian, F. and Behmanesh, I. "Evaluation of FEMA-440 for including soil-structure interaction", *Earthquake Engineering and Engineering Vibration*, **9**(3), pp. 397–408 (2010). https://doi.org/10.1007/s11803-010-0024-2
37. Sarcheshmehpour, M., Estekanchi, H.E., and, Ghannad, M.A. "Optimum placement of supplementary viscous dampers for seismic rehabilitation of steel frames considering soil-structure interaction", *The Structural Design of Tall and Special Buildings*, **29**(1), e1682 (2020). https://doi.org/10.1002/tal.1682
38. Zhang, R., Zhang, L., Pan, C., et al. "Generating high spectral consistent endurance time excitations by a modified time-domain spectral matching method", *Soil Dynamics and Earthquake Engineering*, **145**(5), 106708 (2021). https://doi.org/10.1016/j.soildyn.2021.106708
39. Shayanfar, M., Hatami, A., Zabihi-Samani, M., et al. "Simulation of the force-displacement behavior of reinforced concrete beams under different degrees and locations of corrosion", *Scientia Iranica*, **29**(3), pp. 964–972 (2022). https://doi.org/10.24200/SCI.2021.55422.4214

Biographies

Farzam Moghadam-Rad received his BSc degree in Civil Engineering from Tehran University in 2002. His MSc degree in Earthquake Engineering was obtained from Science and Research Branch of Islamic Azad University in 2005 and now, he is a PhD candidate at the mentioned university. He has a teaching position at the Parand Branch of Islamic Azad University and Engineering system organization. His areas of research include masonry and concrete structure design and execution, wavelet analyses, and active and semi-active control.

Panam Zarfam received his PhD of Structure Engineering from Sharif University. He is a Professor in Civil Engineering at the Department of Structural Engineering, Science and Research Branch of Islamic Azad University where he has taught several graduate and undergraduate courses and supervised many PhD and master students. His areas of research include structure design, nonlinear analysis, seismic design, and active and semi-active control.

Masoud Zabihi-Samani is an Assistant Professor in the field of Structural Engineering. He received his PhD degree from Iran University of Science and Technology in 2014. He is a Professor at and a faculty member of the Civil Engineering Department, Parand Branch of Islamic Azad University where he has taught several graduate and undergraduate courses and supervised 4 PhD students and more than 40 master students. His areas of research include vibration control of structural systems, time endurance method, active & semi-active control, system identification, wavelet & curvelet analysis, and corrosion in concrete structures, in which he has published more than 60 peer-reviewed journal and conference papers nationally and internationally.